Synchronised WindScanner Field Measurements of the Induction Zone Between Two Closely Spaced Wind Turbines

Anantha Padmanabhan Kidambi Sekar, Paul Hulsman, Marijn Floris van Dooren and Martin Kühn

April 11, 2024

Reviewer 1

I would like to thank the authors for providing a thorough answer to my questions and comments. The authors added a description of the terrain and a discussion about the potential impact of the ground heterogeneities on the measured wind speed in the induction zone of the WT2 wind turbine.

Thank you for the feedback and the thorough evaluation of our manuscript. Comments to the reviewer points are made in blue while modifications to the manuscript are shown in red. We hope these changes will positively benefit the manuscript.

Main Comments

Comment 1: In Fig. 12 the authors present measurements of the induction zone of the WT2 wind turbine when the upstream wind turbine was not operating. Based on a visual inspection of that figure, one can observe differences of the inflow wind speed of up to 10% between the y/D>0 and y/D<0 sides. Similar differences are visually observed in Fig. 15 and 16. Furthermore, the wake center in Fig. 15 is not aligned to the center of the rotor, which also introduces an asymmetry to the spanwise profile. For this reason, I do not see how the data presented here reveal a horizontal asymmetry of the longitudinal profile that is a result of the interaction between the strong shear and the wake as the authors suggest. I mention this since the observed asymmetry is highlighted as one of the findings of this study in the abstract and in the conclusions section. I suggest that the authors should comment in the manuscript why they think that the impact of the heterogeneity of the terrain on the flow, which is presented in Fig. 12, is not sufficient to explain the differences presented in Fig. 15.

Reply:

Indeed, the presence of the treeline is expected to cause a perturbation of the flow. While measurements of the undisturbed induction zone showed indications of the impact of the terrain heterogeneity, the additional perturbations induced due to the WT1 wake will additionally influence the flow evolution in the WT2 induction zone. Further differences in the wake profiles can be expected, not only from the impact of the treeline and the WT1 wake but also from the differences in the inflow conditions between the undisturbed and fully waked cases. For the full wake case, the inflow is characterised by high shear ($\alpha = 0.38$) and 19° veer between the top and bottom rotor blade tips. This is in contrast to the undisturbed inflow where a relatively weak shear of $\alpha = 0.21$ was present with a 2° wind veer. Therefore, for the fully waked inflow case, the interaction of the strongly sheared inflow with veering wind into WT2 with the WT1 wake can affect the velocity distribution in the wake profiles, for instance, by promoting mixing between the low and high momentum regions of the rotor [1, 11]. However, due to the large measurement uncertainty, the asymmetric profiles lie within the uncertainty bounds, complicating the interpretation to determine significant flow features, especially in waked measurements.

We have made the following changes in the revised manuscript:

- We have removed the mention of asymmetric induction zone in the abstract and the conclusions.
- In the revised manuscript, we report the asymmetrical velocity distribution in the undisturbed induction zone in Section 3.2.1 and Section 3.2.2, report the possible causes and discuss that the magnitude of the velocity deviations in the horizontal velocity profiles lie within the calculated uncertainty bounds.
- The following text has been added to Section 3.2.2 L506-L514: "The lateral velocity profiles at different upstream positions exhibit a slight asymmetry. While terrain heterogeneity could explain some of the measured features, further differences with the undisturbed inflow case is expected due to the WT1 wake and differences in inflow conditions. For Case 2, the inflow is characterised by high shear and veer between the top and bottom rotor blade tips, in contrast to Case 1. This interaction of vertical shear with the wake can lead to an asymmetric velocity distribution as the wake rotation due to difference in wake convection speeds between the upper and lower rotor halves enhances mixing between the low and high momentum regions of the wake [6, 11, 1]."
- The discussion section (Section 4) is updated to refer to literature which addresses similar observations. Further, the limitations of error analysis for the field measurements is discussed along with recommendations for further measurement campaigns to mitigate limitations of the present study.

Specific Comments

Comment 1 — Lines 451 – 453. Is it possible to add the induction factor value used in Fig. 14?

Reply: L459: We have added the value of the induction factor ($a = 0.23$) used for the estimation of the induction zone deceleration along the rotor axis in Fig. 13 of the revised manuscript.

Technical Corrections

Comment 1 — Lines 329 - 330: "A good qualitative agreement between . . . is noted . . . "

Reply: We have changed this in the revised manuscript.

Comment 2 — Lines 511 – 513. Please add the degree symbol after the values of the yaw misalignment

Reply: We have gone through the revised manuscript and added any missing units to variables.

Reviewer 2

Thanks for implementing the suggested changes. The statistical uncertainty part needs additional work, as shown below.
The main criticality, however, remains the fact the calculated uncertainty bounds are far larger than some difference observed in the mean velocity fields. The justification that the error due to the vertical velocity may be overestimated is not compelling. Generally, one provides a maximum error value to estimate a cap to the uncertainty and show that "despite the error being over estimated the uncertainty is below the acceptable value etc..." This is not the case for this work where a lot of speculations are made to interpret differences in the mean flow way smaller than the uncertainty bands. Please remove all those parts discussing effects that do not pass the uncertainty test such as the non-symmetric induction zone. The paper is already quite long and the readers will benefit from the improved conciseness.

Thank you for the feedback and the thorough evaluation of our manuscript. We acknowledge that the combination of the measurement challenges at the test site and instrumentation limitations led to a large uncertainty in measuring complex flow interactions between the closely spaced turbines. This required a detailed analysis of the associated lidar errors and uncertainties for interpretation of the measurements which was addressed through the high-fidelity simulation approach. The large uncertainty bands resulting from the uncertainty analysis greatly impact how the measurements are interpreted. Therefore, we recognise the validity of the reviewers comments on the interpretation of the field measurements and have reworked the paper to exclude interpretations that lie within the uncertainty bands of the measurements.
The following changes are made:

- References to the symmetrical induction zone:
  - We have removed the description of the asymmetrical induction zone from the abstract and conclusions
  - Section 3.2.1 (L435-455): We report the asymmetrical velocity distribution in the undisturbed induction zone measurements and discuss that the magnitude of the velocity deviations in the horizontal velocity profiles lie within the calculated uncertainty bounds.
  - Section 3.2.2 (L506-L514): We report a asymmetrical velocity distribution in the fully waked induction zone measurements and discuss the difference in the inflow conditions (wind veer and wind shear) that can possibly skew the structure in the spatial distribution of the wake profiles with reference to literature.
  - Section 3.2.3, including Figs. 18, 19 (of the previous revision), the analysis of the induction profiles at 6 spanwise positions for the wake steering cases has been removed as the described effects lie within the uncertainty bounds of the measurements.
  - In the discussion section, only literature is referred which addresses similar observations.The limitations of error analysis for the field measurements is discussed along with recommendations for further measurement campaigns to mitigate limitations of the present study.

- To reduce the length of the paper, we have removed Section 3.1.3 describing the dual-Doppler propagated uncertainty in field measurement and summarised it in Section 3.2.
- An extended statistical uncertainty analysis is presented in Section 3.1.1 based on the requested main corrections.

With these changes, we hope to have addressed the main concern of the reviewer on the interpretation of the measurements and condensed the paper sufficiently to benefit the reader.

New Comments

Comment 1 — Figure 7: please use either always percentage errors (e.g 5%) or non-dimensional error (e.g 0.05).

Reply: As suggested by Reviewer 3, we now show the absolute magnitude of the errors for both the longitudinal and lateral component.

Comment 2 — L 570: "A deeper analysis into the propagated uncertainties indicated that the error in the u,v component estimation was primarily because of the volume averaging effect, beam-intersection angles and beam-pointing errors while the w = 0 m/s assumption was the most dominant source of error. ": so are the volume averaging, beam angles and pointing accuracy the main sources of error, or is it the vertical velocity assumption?

Reply: We have changed this in the revised manuscript.
"A deeper analysis of the propagated uncertainties indicated that the main contribution to the uncertainty to estimate the u, v component was the $w = 0$ m/s assumption. Other important sources of the uncertainty were the probe volume averaging effect, the inaccuracy of the beam-intersection angles and the beam-pointing errors. "

Comment 3 — L 665: please remove that this paper shows how one "should analyse" field as it sounds too bold

Reply: We have removed this in the revised manuscript. It now reads:
"The study further highlights the challenges in conducting field measurements, and the additional considerations needed to characterise the induction zone behaviour."

Main Corrections

Comment 1:

Thanks for adding some statistical uncertainty quantification. This is however not enough for two reasons:

- The use of $\frac{1.96\sigma}{\sqrt{N}}$ is not justified. This simple formula relies on the assumptions of large N (central limit theorem and use of estimator instead of true variance) and independent samples. While the 71 scan repetition can be considered a large enough sample size, in turbulent flows the samples are never independent due to presence of a non-0 integral time scale. Please ensure that the scan repetition time is slow enough to assume that the samples are separated in time by several integral time scales.

- In the conclusion, it is stated that the statistical uncertainty is smaller than the uncertainty of dual Doppler. Statistical uncertainty indeed seems to be ignored after section. Statistical uncertainty being smaller does not mean negligible however, as its magnitude is still a few percent of the freestream velocity. Please add the statistical uncertainty also to the experimental results. It is usually ok to consider it independent from the instrumental uncertainty to that it can be squared-sum to the propagated uncertainty already present in the paper

Reply:

- We acknowledge that we have not provided any justification for the usage of the statistical uncertainty formula. Indeed the utilisation of $\frac{1.96\sigma}{\sqrt{N}}$ requires a large sample size and that the measurement samples are independent of each other. To analyse the independence of the measurement samples, we first calculate the integral timescale (T_i) based on the auto-correlation of the wind speed time series for all presented cases following Cheynet et al [4]. The T_i for the field measurements is calculated from the longitudinal velocity measurements from the hub height anemometer mounted on the met mast. Figure 1 illustrates the auto-correlation function for the measurements and simulations.

  The T_i is obtained by integrating the auto-correlation function till the first-zero crossing and

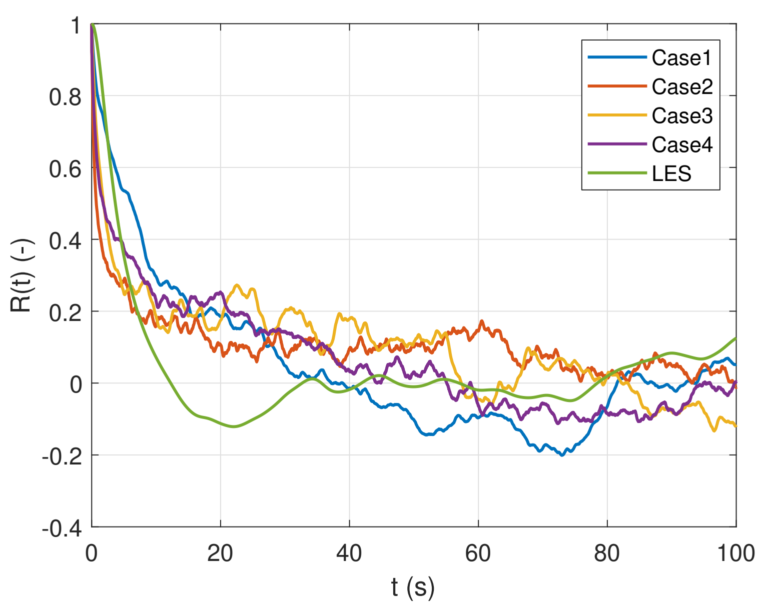

Figure 1: Plot of the autocorrelation function of the five cases. The LES data was extracted at the location $x/D = -0.75, y/D = 0, z = 136$ m.

tabulated in Tab 1. It should be noted that the time scales for the field cases could differ from the time scales present in the scanning area due to the separation between the met mast and the scan area. Furthermore, the presence of the WT1 wake in Cases 2, 3, and 4 will reduce the time scales present in the scanning area due to increased turbulence in the near wake depending on the evolution of the turbulent eddies in the wake.
For all cases, the integral length scale is smaller than the scan repetition rate by a factor of at least 2. Henk and Lumey [5] describe that, for statistical independence, sampling the wind once every two integral time scales is adequate. Therefore, while the measurements may not be entirely independent due to the relatively short integral time scale compared to the scanning time, they may still be treated as approximately independent.
We now calculate the statistical uncertainty using $\frac{1.96\sigma}{\sqrt{N_s}}$ to estimate the statistical uncertainty where N_s is the number of independent sample size. This effective sample size accounts for correlations in the turbulent flow, leading to a more accurate estimate of the error of the mean in comparison to the number of measured samples and is calculated as:

$$N_s = N\langle\frac{1-r}{1+r}\rangle \tag{1}$$

Where r is the lag-1 auto correlation [9]. The effective sample sizes are presented in Tab 1 and subsequently used for calculating the statistical uncertainty.

We have added the following information to the revised manuscript:

- We have updated Table 3 describing the inflow conditions with the integral time scales provided in Table 1 .
- Revised Section 3.1.1 to include the method for estimation of independent sample size that is thereafter used for statistical uncertainty estimation.

Case	T_i (s)	Scan time multiples	N	N_s
1	9.4	3.1	107.4	95.4
2	10.5	2.8	52.7	41.1
3	11.1	2.6	70.9	25.5
4	9.10	3.2	64.8	44.7
LES	4.5	6.5	71.0	64.7

Table 1: Estimations of the integral time scale (T_i), number of measured samples (N) and the number of independent samples N_s for the field measurements and the LES.

- Assuming a perfectly calibrated lidar system with no measurement bias and uncorrelated errors, we have added the statistical uncertainty to the propagated uncertainty through the squared sum approach to estimate the total combined uncertainty. The total combined uncertainty accounts for the statistical variability in the measured flow in addition to the variability due to the lidar limitations.

  - Revised Section 3.1.2 on how the total combined uncertainty was estimated. "The shaded region illustrates the total measurement uncertainty where the statistical uncertainty and the propagated uncertainty are summed in quadrature assuming a perfectly calibrated lidar with no measurement bias and uncorrelated errors. The total combined uncertainty accounts for the statistical variability in the measured flow in addition to the variability due to the lidar limitations."

– Figures 10, 12, 13, 15, 17 of the revised manuscript are now updated to show the total combined measurement uncertainty.

Technical Corrections

Comment 1 — 6: The comment was more intended to point out the missing justification for the values of z/L used to define the stability classes. More specifically, why is $z/L < 0.4$ chosen as the neutral class?

Reply: Thank you for the clarification. The stability classification was provided in the paper following the free field lidar experiments of Simley et al., [7] who had also used the z/L parameter to characterise stability for their WindScanner measurements. We have further corrected a typo whereby neutral conditions is selected for $-0.04 \leq z/L \leq 0.04$.
"The stability classification of the Obhukov parameter z/L is performed for 30-minute averages based on Wyngaard [10] and further used in Simley et al [7], where negative values indicate the presence of unstable conditions ($z/L \leq -0.04$), positive values ($z/L \geq 0.4$) correspond to stable conditions, and values close to zero ($-0.04 \leq z/L \leq 0.04$) are related to neutral conditions. "

Comment 2 — 11: The error on the location was not corrected in the new version, there is still $x/D = 0.16$

Reply: In the revised manuscript we have indicated that the profiles are extracted at $x/D =$ -0.08 in alignment with the horizontal profiles plotted in Fig. 10.

Comment 3 — 12: please add that stable stratification also suppressed vertical displacement of air parcels thus enhancing flow blockage as possible explanation of the stronger induction

Reply: We have changed this in the revised manuscript to the following:
"This strong velocity deficit can be attributed to high axial induction and weakly stable stratification during the measurement period inhibiting vertical displacement of air particles further enhancing the blockage. "

Comment 4 — 3: Thanks for pointing out Bastankhah's explanation for this asymmetry. In the text, it should be made clearer that this is a dynamic aerodynamics or stall effect, but that the angles of attack are perfectly symmetric in a quasi-static sense

Reply: We have changed this in the revised manuscript to the following:
"This asymmetry can potentially be attributed to the dynamic interaction between the vertical shear and the rotating blades, which was noted by [2] using wind tunnel measurements."

Comment 5 — 15: every time the "uncertainty bounds" are cited in the text, the confidence level should be mentioned too. E.g. 1.96 σ would correspond to 95% confidence level if Gaussianity is assumed, and so forth

Reply: We have added the following text to Section 2.3.2 of the revised manuscript:
"All the uncertainty terms in the paper are the 1.96 σ values of the corresponding error distributions; i.e. they are expected to include 95 % of all values."

Comment 6 — 24: it is still confusing. It is first stated that the $y/D < 0$ sides shows faster deceleration. This implies for positive yaw offset, more deceleration in the freestream, for the negative yaw offset more deceleration in the wake. Then is it stated that for the negative offset "similar effects of the induction are seen where the wake at $y/D < 0$ decelerated faster compared to the freestream" which is in contradiction with what happens for the positive offset where the freestream part has stronger deceleration

Reply: We have removed the spanwise induction figures and explanation in the revised manuscript as described earlier as the measured flow features are within the uncertainty bounds of the measurements.

Reviewer 3

Summary: The study presents measurements of the flow between two closely spaced wind turbines using a ground-based dual Doppler lidar setup. Four data sets for a fully waked inflow (with wake steering), a partially waked inflow, and an undisturbed inflow are described and discussed in detail. Additionally, a detailed error study is presented including a LES simulation of the setup to investigate the dual-Doppler lidar reconstruction errors. The case study is quite interesting, because the near wake and the induction zone have seen much less attention in literature than the far wake – especially from field measurements.

General comments I have not detected any major flaws with the manuscript. My specific comments below mostly concern a more precise description of the methods. I also noticed several instances of missing words, wrong sentence structures, or one-sentence paragraphs and I recommend that the authors iterate the manuscript more to improve this aspect.
The replies of the authors to the comments of the reviewers are mostly satisfactorily in my opinion.

We thank the reviewer for their critical assessment of our work with general and specific comments. The revised manuscript has been carefully proofread for spelling and grammar errors. In the following section, we address the specific comments point by point. Comments to the reviewer points are made in blue while modifications to the manuscript are shown in red. We hope these changes will positively benefit the manuscript.

Specific Comments

Comment 1 — Line 50-51: A sentence introducing Doppler lidars could be added here.

Reply: We have changed this in the revised manuscript to:
"Lidars are capable of measuring the velocity through the Doppler shift remotely and provide a way to measure the flow around wind turbines in the field [8]."

Comment 2 — Line 172: If the x-axis is the connecting line between the two turbines and only wind directions approximately parallel to it are considered, then the y-axis should be pointing in the lateral direction and not the longitudinal direction.

Reply: We have changed this in the revised manuscript:
"The measurements are visualised in a global fixed reference frame centred at the bottom of WT2, where the x-axis is the connecting line between the two turbines, and the $y-$ and $z-$ axes are positive to the right looking towards WT2 and in an upward direction."

Comment 3 — Line 187: "met mast hub height" is not quite clear.

Reply: We have changed this in the revised manuscript:
"We rotated all measurements in the global reference frame into the main wind direction measured at the met mast at 1 m below WT1 hub height"

Comment 4 — Line 259: The filtering method for hard targets is not described in the manuscript, but data at the rotor plane is used later (e.g. Figure 12). How where the measurements affected by hard-targets identified and discarded?

Reply: The dynamic filtering method from Beck and Kühn [3] filters for the line-of-sight velocity and the signal quality in a bi-variate manner based upon the assumption of self-similarity of valid data. Plotting the LOS and signal quality (SNR) together, clusters of data points corresponding to the measurements and hard targets such as moving blades, clustered at different levels of signal quality can be identified owing to their differing signal quality and hence are removed. It is noted that the filtering is applied on the LOS measurements collected over the entire scanning area for the duration of the measurements. Hard targets such as the nacelle could be easily identified from the LOS-SNR distribution while the filtering of the blade interference is dependent on the blade azimuthal angle.
We could plot the data at the rotor plane as the measurements are presented as averages for the total measurement duration and valid measurements could be recorded at the rotor plane when devoid of blade interference.
We have added the following text in Section 3 L291-L297:
"Data filtering for the field measurements was performed using a kernel density-based filter based on [3] to identify and remove low-quality measurements. The method filters for the line-of-sight velocity and the Signal-Noise-Ratio in a bi-variate manner based upon the assumption of self-similarity of valid data. The method is applied on all the collected v_{vlos} measurements on the measurement plane and is capable of identifying hard targets such as the nacelle and blades through the clusters in the v_{vlos}-SNR space. The measurements are discretized and grouped into bins based on their v_{vlos}- SNR values. The frequency distribution of data points within each bin was then determined. Bins with frequencies exceeding 20 % of the most populated bin were retained for further analysis. "

Comment 5 — Table 3: Caption does not mention the ± term for the wind direction. I assume it is the standard deviation?

Reply: The ± term indicates standard deviation of the wind direction. The table caption has been updated.

Comment 6 — Is it the gradient of the temperature or the potential temperature?

Reply: The gradient refers to the potential temperature gradient. We have updated the revised manuscript with this information.

Comment 7 — Figure 7 / Reply to Reviewer 2, Comment 2: Normalizing the statistical uncertainty of the v-component with the longitudinal wind speed might be misleading, because the resulting percentage values are not useful as a relative error of the lateral velocity. Showing the non-normalized uncertainty should be considered for the lateral velocity

Reply: Thank you for this comment. We now show the un-normalised longitudinal and lateral velocity error in Figures 7, 8.

Comment 8 — Line 442: Please specify to which fit is referred here

Reply: Thank you for pointing this out. We wanted to refer to the fact that due to low data return, the velocity along the rotor axis was not plotted behind the rotor.
We have rephrased the sentence to:
"Data availability between $0 \leq x/D \leq 0.2$ is reduced due to the presence of the nacelle and therefore excluded."

Comment 9 — Line 492: For consistency of language, using "lateral velocity" instead of "spanwise velocity" would be better (I believe all previous instances used lateral velocity for v)

Reply: We have replaced the term "spanwise velocity" with "lateral velocity" throughout the revised manuscript.

Comment 10 — Line 502-506: Aside from the yaw difference between Case 3 and Case 4, there is also a 10° wind direction difference. For Case 3, the average wind direction is 217° and a wake that is offset to the left from the WT1-WT2 line would be expected from this as well. Is the found difference in wake deflection between the two cases larger than what would be expected for "straight wakes" for a 10° difference in wind direction alone?

Reply: The 10° difference from the WT1-WT2 line for Case 3 would influence the wake from WT1 and move it further left of WT2 looking downstream. The additional positive yaw offset at WT1 will further deflect the wake in this direction. This is supported by the location of the wake for the positive yaw case at y/D = 0.32 in comparison to the wake being present at y/D = -0.20 in the negative yaw case.
In a scenario where the two turbines operate with a 10° difference in wind direction from the WT1-WT2 line without any wake steering applied on WT1, it is expected that the wake will not be deflected further to the left in comparison to when wake steering is applied. However, we cannot provide a definitive answer as the wake behaviour is highly dependant on the inflow and turbine conditions and such a wake case with a 10° offset between the 228° line and the wind direction while the turbines were operating in a straight wake case was not measured.
We have made the following changes to the manuscript:
For clarity, Figure 16 in the revised manuscript has been updated to show the average wind direction during the positive and negative wake steering cases.

Comment 11 — Line 506-507: Along the same line as above, I wonder what the impact of different wind directions is on lateral velocity component. Because the coordinate system was defined along the WT1-WT2 line and not parallel to the wind direction, the wind direction offset from the x-axis will be projected into the lateral velocity. Can this be quantified and is it smaller than the observed difference in lateral velocity between the two cases?

Reply: Yes, due to our definition of the coordinate system where the x-axis is aligned to the WT1-WT2 line at a heading of 228°, any changes in wind direction would be projected onto the velocities on the scanning area. This would be in addition to the lateral velocity magnitude measured in the defined coordinate system in comparison to the aligned case. This can be already seen in Fig 17 top right, where the v component magnitudes are much larger in comparison to the relatively more aligned negative steering case. A preliminary quantification can be provided by calculating the addition to the

lateral velocity component as $u_\infty \sin(\Phi)$ where u_∞ is the wind velocity and Φ is the offset from the WT1-WT2 line. Therefore, for the 10° offset case, approximately 17% of the wind magnitude will be projected into the lateral component.
For cases 3 and 4, this value is still slightly smaller than the observed differences in the lateral velocities between the two cases across the scanning area.
We have made the following changes to the manuscript at L525-L528:
"In both cases, the maximum magnitude of the lateral velocity inside the deflected wake is approximately $0.2\ u_\infty$ to $0.25\ u_\infty$. The positive yaw offset case exhibits a comparatively more substantial lateral flow component compared to the negative yaw offset due to the 10° misalignment between the turbine orientation and the wind direction as the lateral velocity would be increased by the projection of misaligned inflow into the defined coordinate system."

Comment 12 — The reply to Reviewer 1, Comment 4 seems to support that an assumed line-of-sight velocity accuracy of 0.1% is too low. Would the results hold for the more realistic 2% error? Or can a threshold be provided until which the results hold?

Reply: To estimate the error in the 2D velocity estimation for a range of line-of-sight errors $(e_{\mathrm{vlos},1}, e_{\mathrm{vlos},2})$ we use the SUP methodology described in Eqns 7, 8 in the revised manuscript applied on the LES wind field.

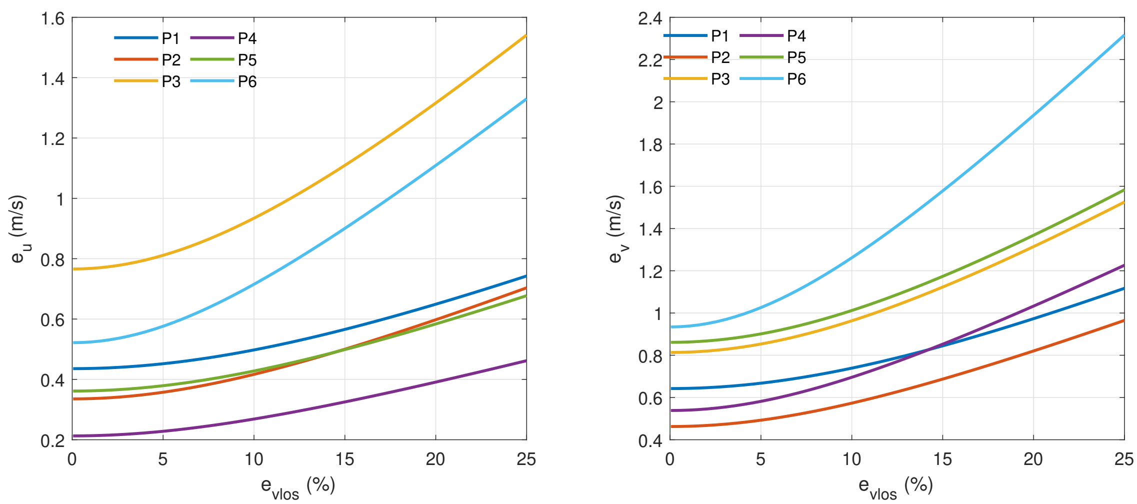

Figure 2: Variation of e_{u} and e_{v} to e_{vlos} at locations P1 to P6 in the LES wind fields.

Figure 2 shows the variation of v_{los} contribution to the u and v component error for a range of v_{los} errors from 0.05 % to 25 % assuming same e_{vlos} for both lidar systems. The results are shown for 6 spatial locations P1...P6 distributed over the scanning area as described in Section 3.1.2 of the revised manuscript. The spatial variations of $e_{\mathrm{u,v}}$ at the different locations is due to the variations in the w components and beam scanning angles contributing to the total error.
At each spatial location, $e_{\mathrm{u}}, e_{\mathrm{v}}$ does not show large variations between e_{vlos} of 0.1 % utilised in the paper and a realistic 2 % error requested by the reviewer. Both $e_{\mathrm{u}}, e_{\mathrm{v}}$ show larger sensitivity to higher e_{vlos} simply due to the magnitude of the line-of-sight error becoming larger than the other error sources $(e_{\mathrm{w}}, e_\chi, e_\delta)$. Therefore, the presented results will hold for a more realistic 2% v_{los} error.
We have added the following in Section 4 Discussion of the revised manuscript:

Further WindScanner simulations indicated that the total propagated error was insensitive to a higher and more realistic 2 % line-of-sight error.

Technical Comments

Comment 1 — Line 127: I believe "scanner head" is more common than "scan head".

Reply: We have changed this in the revised manuscript.

Comment 2 — Eq. (1): Comma instead of full stop.

Reply: We have changed this in the revised manuscript.

Comment 3 — Line 145: The u and v variables were already introduced in line 140.

Reply: We have changed this in the revised manuscript to the following:
"The u, v velocity components can be resolved by an additional assumption of the vertical flow component and combining the two v_{los} measurements by dual-Doppler wind field reconstruction by solving Eq. (2)."

Comment 4 — Line 204: Insert "it" in "as is"

Reply: We have changed this in the revised manuscript.

Comment 5 — Line 211-212: Sentence structure (remove first and).

Reply: We have changed this in the revised manuscript.

Comment 6 — Line 220: Remove "a" in "until a multiple scans".

Reply: We have changed this in the revised manuscript.

Comment 7 — Line 290: Either plural for performance or replace "were" with "was".

Reply: We have changed this in the revised manuscript.

Comment 8 — Line 360: No new paragraph here.

Reply: We have removed the single line paragraph and added it to the next paragraph.

Comment 9 — Line 500: No new paragraph.

Reply: We have removed the single line paragraph and added it to the next paragraph..

References

[1] M. Abkar, J. N. Sørensen, and F. Porté-Agel. An Analytical Model for the Effect of Vertical Wind Veer on Wind Turbine Wakes. *Energies 2018, Vol. 11, Page 1838*, 11(7):1838, 7 2018.

[2] M. Bastankhah and F. Porte-Agel. Wind tunnel study of the wind turbine interaction with a boundary-layer flow: Upwind region, turbine performance, and wake region. *Physics of Fluids*, 29(6), 2017.

[3] H. Beck and M. Kühn. Dynamic Data Filtering of Long-Range Doppler LiDAR Wind Speed Measurements. *Remote Sensing*, 9(6):561, 6 2017.

[4] E. Cheynet, J. B. Jakobsen, J. Snæbjörnsson, T. Mikkelsen, M. Sjöholm, J. Mann, P. Hansen, N. Angelou, and B. Svardal. Application of short-range dual-Doppler lidars to evaluate the coherence of turbulence. *Experiments in Fluids*, 57(12):1–17, 12 2016.

[5] Henk Tennekes and John L. Lumley. *A First Course in Turbulence.* The MIT Press, 2018.

[6] N. Sezer-Uzol and O. Uzol. Effect of steady and transient wind shear on the wake structure and performance of a horizontal axis wind turbine rotor. *Wind Energy*, 16(1):1–17, 1 2013.

[7] E. Simley, N. Angelou, T. Mikkelsen, M. Sjöholm, J. Mann, and L. Y. Pao. Characterization of wind velocities in the upstream induction zone of a wind turbine using scanning continuous-wave lidars. *Journal of Renewable and Sustainable Energy*, 8(1):013301, 1 2016.

[8] C. Werner and J. Streicher. Lidar: Range-Resolved Optical Remote Sensing of the Atmosphere. 102, 2005.

[9] D. S. Wilks. Statistical Methods in the Atmospheric Sciences, Fourth Edition. *Statistical Methods in the Atmospheric Sciences, Fourth Edition*, pages 1–818, 1 2019.

[10] J. C. Wyngaard. *Turbulence in the Atmosphere.* Cambridge University Press, Cambridge, 2010.

[11] S. Xie and C. L. Archer. A Numerical Study of Wind-Turbine Wakes for Three Atmospheric Stability Conditions. *Boundary-Layer Meteorology*, 165:87–112, 2017.